Feed-forward information and zero-lag synchronization in the sensory thalamocortical circuit are modulated during stimulus perception

Adrià Tauste Campo[a,b,1], Yuriria Vázquez[c,d], Manuel Álvarez[c], Antonio Zainos[c], Román Rossi-Pool[c], Gustavo Deco[b,e], and Ranulfo Romo[c,f,1]

[a]Barcelonaβeta Brain Research Center (BBRC), Pasqual Maragall Foundation, 08005 Barcelona, Spain; [b]Center for Brain and Cognition, Department of Information and Communication Technologies, Universitat Pompeu Fabra, 08003 Barcelona, Spain; [c]Instituto de Fisiología Celular–Neurociencias, Universidad Nacional Autónoma de México, 04510 Mexico City, Mexico; [d]Laboratory of Neural Systems, The Rockefeller University, New York, NY 10065; [e]Institució Catalana de Recerca i Estudis Avançats, 08010 Barcelona, Spain; and [f]El Colegio Nacional, 06020 Mexico City, Mexico

Contributed by Ranulfo Romo, February 20, 2019 (sent for review November 8, 2018; reviewed by Sonja Grün and Stefano Panzeri)

The direction of functional information flow in the sensory thalamocortical circuit may play a role in stimulus perception, but, surprisingly, this process is poorly understood. We addressed this problem by evaluating a directional information measure between simultaneously recorded neurons from somatosensory thalamus (ventral posterolateral nucleus, VPL) and somatosensory cortex (S1) sharing the same cutaneous receptive field while monkeys judged the presence or absence of a tactile stimulus. During stimulus presence, feed-forward information (VPL → S1) increased as a function of the stimulus amplitude, while pure feed-back information (S1 → VPL) was unaffected. In parallel, zero-lag interaction emerged with increasing stimulus amplitude, reflecting externally driven thalamocortical synchronization during stimulus processing. Furthermore, VPL → S1 information decreased during error trials. Also, VPL → S1 and zero-lag interaction decreased when monkeys were not required to report the stimulus presence. These findings provide evidence that both the direction of information flow and the instant synchronization in the sensory thalamocortical circuit play a role in stimulus perception.

behaving monkeys | somatosensory thalamocortical circuit | tactile detection task | simultaneous single-unit recordings | directed information-theoretic measure

A major challenge in systems neuroscience involves understanding how perceptual experiences arise from coordinated neural activity, and how functional information flows among the interacting neurons (1–5). The sensory thalamus is an essential node within the perceptual circuit, relaying stimulus information from the periphery to cortex (6). Given the connectivity between the thalamus and cortex, feed-back corticothalamic inputs could modulate feed-forward thalamocortical stimulus information transmission during perception (7–10). Thus, the thalamus could act as a processing unit in continuous interaction with the cortex (6, 11, 12). Evidence supporting this view comes from previous studies in anesthetized (13–15) and awake animals (10, 16). However, it is unclear how feed-forward and feed-back information flows coexist within the thalamocortical circuit and whether they correlate with the subject's perception.

To address these questions, we recorded the simultaneous activity of single neurons in the ventral posterolateral nucleus (VPL) of the somatosensory thalamus and in primary somatosensory cortex (S1) sharing the same cutaneous receptive field while monkeys performed a vibrotactile detection task. The animals were trained to report the presence or absence of a tactile stimulus of variable amplitude. In this task, previous work showed that VPL and S1 neurons encode mostly the physical features of the stimulus (17, 18). These findings raise several questions. First, how is sensory information communicated between the VPL and S1 at the level of single neurons? Second, what is the balance between the information flowing in a feed-forward direction (VPL → S1) and in a feed-back (S1 → VPL) direction? Third, does the information flow between VPL and S1 correlate with the subject's perception?

In the current work, we addressed the above questions by detecting time-varying directional couplings between the recorded VPL and S1 neuron pairs across many trials as a measure of the functional thalamocortical information flow needed to perform a vibrotactile detection task. During the stimulus presence, feed-forward (VPL → S1) information largely prevailed over feed-back (S1 → VPL) information. Interestingly, zero-lag interactions emerged with the stimulus amplitude above detection threshold, suggesting the existence of cortical common inputs facilitating the transmission of stimulus information. Critically, at the stimulus onset, feed-forward information correlated with the subject's perception. During a variant of the detection task (passive condition, in which no response was required from the animal), feed-forward information was reduced during the expected stimulation windows of stimulus-present and stimulus-absent trials, while zero-lag interaction was mainly reduced in the first half of the stimulus. Taken together, our results characterize the functional information flow between VPL–S1 neuron pairs during tactile perception. They reveal that besides relaying stimulus information

Significance

The direction of information flow between brain circuits may be key in cognitive functions. We addressed this problem by evaluating a directional correlation measure between simultaneously recorded neurons from somatosensory thalamus (ventral posterolateral nucleus, VPL) and somatosensory cortex (S1) sharing the same cutaneous receptive field while monkeys judged presence or absence of tactile stimuli. During stimulus presence, feed-forward (VPL → S1) information increased as a function of stimulus amplitude, while feed-back (S1 → VPL) information was unaffected. Simultaneously, zero-lag interaction emerged with increasing stimulus amplitude, contributing to thalamocortical synchronization. Furthermore, VPL → S1 information decreased during error trials. Also, both VPL → S1 and zero-lag interactions decreased when monkeys were not required to report stimulus presence. Thus, directional and coordinated information in the thalamocortical circuit is associated with stimulus perception.

Author contributions: A.T.C. and R.R. designed research; Y.V., M.Á., A.Z., and R.R. performed research; A.T.C. and R.R. contributed new reagents/analytic tools; A.T.C., R.R.-P., and G.D. analyzed data; and A.T.C., Y.V., R.R.-P., G.D., and R.R. wrote the paper.

Reviewers: S.G., Research Center Juelich; and S.P., Italian Institute of Technology.

The authors declare no conflict of interest.

[1]To whom correspondence may be addressed. Email: adria.tauste@gmail.com or rromo@ifc.unam.mx.

This article contains supporting information online at www.pnas.org/lookup/suppl/doi:10.1073/pnas.1819095116/-/DCSupplemental.

feed-forward information conveys task-context information, whereas zero-lag interactions might reflect the cortically driven coordinated activity of VPL and S1 that is required for information transmission during task performance.

Results

Two monkeys *(Macaca mulatta)* were trained to perform a tactile detection task (2, 3). In each trial, the animal had to report whether the tip of a mechanical stimulator vibrated or not (Fig. 1*A*). Stimuli were sinusoidal, had a fixed frequency of 20 Hz, and were delivered to the glabrous skin of one fingertip; crucially, they varied in amplitude across trials. Stimulus-present trials were interleaved with an equal number of stimulus-absent trials in which no mechanical vibrations were delivered (Fig. 1*A*). The presence or absence of the stimulus (0.5 s) was preceded by a variable prestimulus period (1.5 to 3 s), followed by a fixed poststimulus delay period of 3 s before the monkey reported its decision by pressing one of two push buttons (Fig. 1*A*). In stimulus-absent trials, we will refer to the possible window of stimulation (PWS) as the temporal windows when the monkeys may expect the stimulus (19). Stimulus detection thresholds were calculated from the behavioral responses (Fig. 1*B*, *Left*). Importantly, depending on the monkeys' responses, trials could be classified into four types: hits and misses in the stimulus-present trials and correct rejections and false alarms in the stimulus-absent condition (Fig. 1*B*, *Right*). Once the animals performed the task at near detection threshold (8 μm), we recorded the simultaneous activity of spike trains from individual neurons from VPL and S1 (areas 3b or 1; Fig. 1*C*) while monkeys performed the task. Here, it is important to highlight that the recorded neuron pairs (n = 84) from the VPL and S1 shared exactly the same cutaneous receptive fields (Fig. 1*D*). Fig. 1*E* qualitatively shows that the neurons of VPL and S1 modulate their firing rate during the stimulus-present condition (Fig. 1*E*, *Left*), but not during the stimulus-absent condition (Fig. 1*E*, *Right*). Thus, it appears an optimal experimental condition for assessing the functional time-varying information flow between neuron pairs from VPL and S1 during the detection task.

Assessing Directional Information Flow Between VPL and S1. It is well-established that the VPL relays information from the skin mechanoreceptors up to S1 (Fig. 1 *C* and *D*). This knowledge allows us to test the following hypothesis in the detection task: After the stimulus onset, the flow of functional information becomes crucially larger in the VPL → S1 direction than in the S1 → VPL direction. However, given the stronger anatomical connectivity from S1 to VPL than from VPL to S1 (12), the second hypothesis is that the flow of functional information is higher from S1 → VPL than from VPL → S1. Importantly, we also hypothesize that the information flow between VPL and S1 could be affected by task conditions (Fig. 1*B*). We addressed all these hypotheses by using a nonparametric method that measures directional information flows between the simultaneously recorded spike trains of pairs of VPL–S1 neurons in single trials and within slicing time windows of 0.25 ms using a directed information-theoretic measure (5, 20, 21) (*SI Appendix*). The method is illustrated in Fig. 2*A*. To measure single-neuron interactions on a fine temporal scale along each task trial, we estimated delayed versions of the directed information-theoretic measure (*SI Appendix*, Eq. **S1**) in both directions (VPL → S1 and S1 → VPL) for every pair of simultaneous VPL–S1 spike trains at the short time delays [0, 2, 4, . . ., 20 ms] (Fig. 2*A*, *Left*). To infer the significance of each estimation, we defined a maximizing-delay statistic (*SI Appendix*, Eq. **S2**) and built the corresponding null distribution using circular shifts of the target spike-train sequences (Y^T), which preserved the firing rate and the short-range (0 to 50 ms) autocorrelation of both spike trains while destroying their temporal alignment (Fig. 2*A*, *Middle*). For

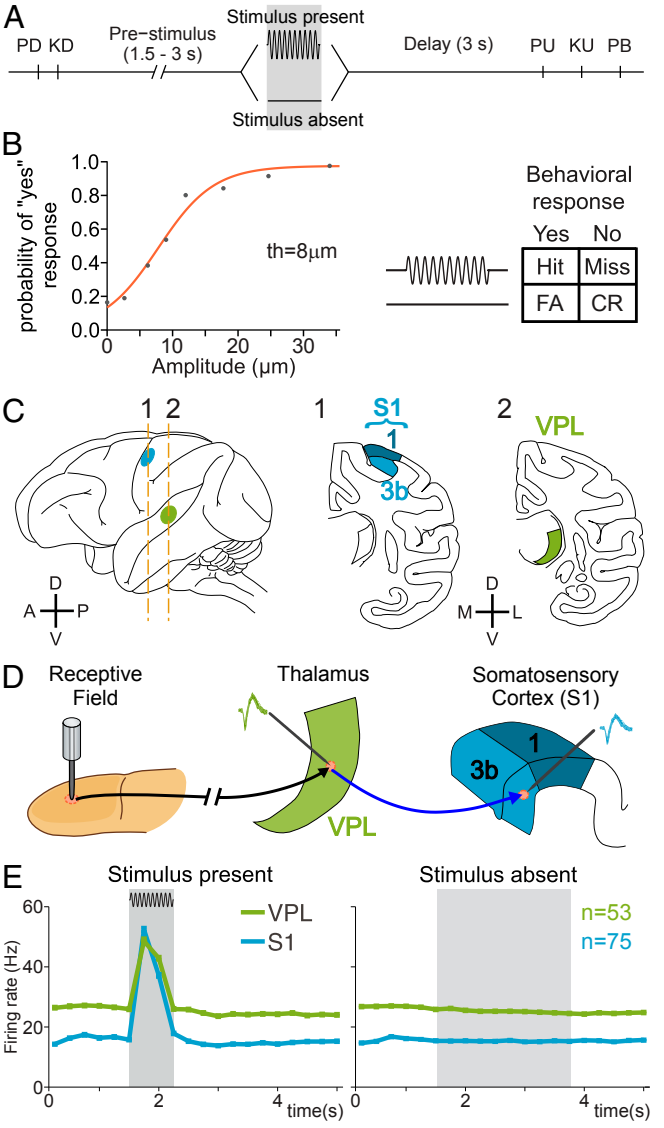

Fig. 1. Detection task, psychophysical performance, recording sites, and neuronal responses during the task. (*A*) Vibrotactile detection task. Trials began when the stimulator probe indented the skin of one fingertip of the monkey's restrained right hand (probe down, PD); the monkey reacted by placing its left, free hand on an immovable key (key down, KD). After a variable prestimulus period (1.5 to 3 s), a vibratory stimulus of variable amplitude (1 to 34 μm, 20 Hz, 0.5-s duration) was presented on one half of the trials; no stimulus was presented on the other half of the trials. Following the stimulus presentation period or a period where no stimulus was delivered, the monkey waited for 3 s until the probe was lifted off from the skin (PU, probe up), then the animal removed its free hand from the key (KU, key up) and pressed one of two push buttons (PBs) to report whether the stimulus was present or absent. Lateral and medial buttons were used for reporting stimulus presence and stimulus absence, respectively. Stimulus-present and stimulus-absent trials were randomly interleaved within a run. (*B*) The button pressed indicated whether the monkey felt the stimulus (henceforth referred as yes and no responses, respectively). (*B*, *Left*) Mean psychometric function depicting the probability of the monkey's reporting yes as a function of the stimulus amplitude (th = 8 μm, detection threshold). (*B*, *Right*) Behavioral responses depending on the stimulus presence (Hit or Miss) or stimulus absence (CR, correct rejection; FA, false alarm). (*C*) Recording sites in the ventral posterior lateral (VPL) nucleus (green) of the thalamus and in areas 1 and 3b of the primary somatosensory cortex (S1, cyan). (*D*) Scheme depicting how the neural activity from single neurons in the VPL and S1 (3b or area 1) sharing the same cutaneous receptive field was simultaneously recorded during the detection task. (*E*) Mean firing rate for the simultaneously recorded VPL (n = 53) and S1 (n = 75) neurons during the stimulus-present and stimulus-absent trials.

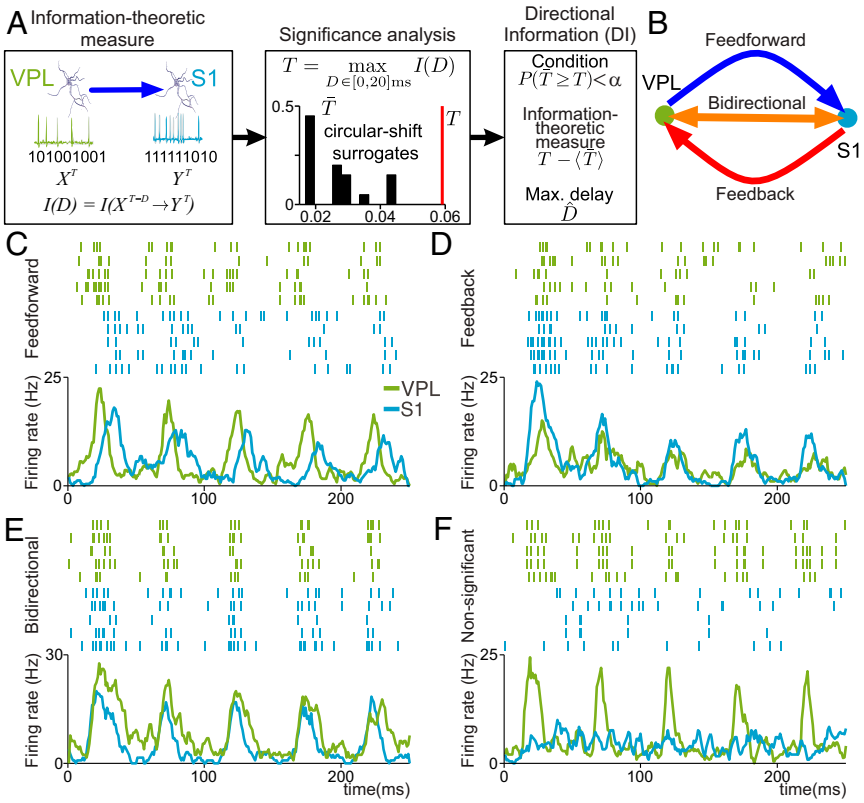

Fig. 2. Assessing DI between pairs of VPL and S1 neurons during the detection task. (*A*) Sequential scheme representing the method to infer DI at single-trial level. (*Left*) Information-theoretic measure is estimated between single-trial spike trains of the simultaneously recorded neurons in VPL and S1 for delays (0, 2, . . ., 20) ms. (*Middle*) Significance is locally determined via nonparametric testing ($\alpha = 0.05$) of a maximizing-delay statistic. (*Right*) Every significant statistic ($P < \alpha$) is associated with an unbiased information-theoretic measure value ($T - \langle T \rangle$) and a maximizing delay ($\hat{D}$). (*B*) Graphical representation for feed-forward (VPL → S1, in blue), feed-back (S1 → VPL, in red), and bidirectional (S1 ↔ VPL, in orange) information between VPL and S1 neurons. (*C–F*) Raster plots and spike density functions depicting the neural activity occurring during the first 250 ms of stimulation (34 μm) for examples of VPL (green) and S1 (cyan) neuron pairs involved in feed-forward (*C*), feed-back (*D*), and bidirectional (*E*) information and nonsignificant (*F*) statistic values.

each directional spike-train pair, (X^T, Y^T), the method assessed the significance of the statistic together with an unbiased estimation of the statistic value and the maximizing delay (Fig. 2*A*, *Right*). Directional spike-train pairs associated with significant estimators ($\alpha = 0.05$) will be referred to as directional information (DI) trials (*SI Appendix*) and will be represented for different experimental conditions as a percentage over the corresponding pairs and trials. Finally, statistical comparisons between percentages were assessed with nonparametric methods (21) and validated via Cohen's *H* (22) effect size (*H*) for proportion differences (*SI Appendix*).

A first characterization of the VPL–S1 simultaneous activity was done by measuring the percentage of DI (*SI Appendix*, Fig. S1*A*) as well as the mean DI value (*SI Appendix*, Fig. S1*B*) for VPL → S1 and S1 → VPL directions during the time course of the detection task for spike trains above a firing rate threshold (35 Hz). Both quantities were calculated separately for the stimulus-present (*SI Appendix*, Fig. S1*B*, *Left*) and stimulus-absent (*SI Appendix*, Fig. S1*B*, *Right*) trials. For the analysis of stimulus-present trials here and in the subsequent figures, we removed the variable-time prestimulus period in every trial and aligned all trials to the stimulus onset time. The analysis showed that for the stimulus-present trials the amount of VPL → S1 DI (trials = 3,216 in neuron pairs = 84, $P < 0.01$, $H > 0.5$, cyan line; *SI Appendix*, Fig. S1*A*, *Left*) was significantly larger than the amount of S1 → VPL DI during the first half (250 ms) of the stimulus period and weaker but still significant during the second half ($H < 0.5$). However, the strongest effect at stimulus onset was not mimicked by the mean DI value ($P < 0.01$, $D < 0.3$; *SI Appendix*, Fig. S1*B*, *Left*). In contrast, for stimulus-absent trials, the greatest differences were manifested by the amount of DI (trials = 4,371 in neuron pairs = 84, $P < 0.01$, $H > 0.3$; *SI Appendix*, Fig. S1*A*, *Right*) during the PWS (1.5 to 3.5 s) with no counterpart evidence from the mean DI value (*SI Appendix*, Fig. S1*B*, *Right*). Despite its moderate statistical effect ($H < 0.5$), *SI Appendix*, Fig. S1 shows a positive gap between VPL → S1 and S1 → VPL directions already during the prestimulus period, which could reflect an underlying directionality imbalance facilitating subsequent sensory information transmission. In conclusion, we restricted our analysis to the percentage of DI (rather than the mean DI value) due to its greater sensitivity to detect directionality differences during the stimulus and possible stimulation windows.

As a first approach, we considered exclusively two directionality cases: VPL → S1 and S1 → VPL (*SI Appendix*, Fig. S1). However, when studying DI flow for two simultaneous spike *T*-length trains X^T and Y^T at a given time interval (e.g., 250 ms) one may instead consider three disjoint cases: The spike trains are coupled in only one direction $(X^T \to Y^T)$, in only the opposite direction $(Y^T \to X^T)$ or simultaneously coupled in both directions $(X^T \leftrightarrow Y^T)$. In principle, these three cases correspond to neurons in each pair taking three different roles—driver, target, or both—which may be associated with distinct functional mechanisms (24). According to this notion, we classified DI estimates by pairing the location and role of each neuron per trial. In short, we defined as feed-forward information (VPL → S1) those DI estimates involving pairs where the neuron of VPL was only driver and the neuron of S1 was only target. Similarly, we

defined as feed-back information (S1 → VPL) where the neuron of S1 was only driver and the VPL neuron was only target. Finally, pairs where the neuron in VPL and the neuron in S1 were simultaneously drivers and targets (at possible different delays) of that interaction were labeled as bidirectional information. Fig. 2*B* shows a schematic representation for the three types of DI and Fig. 2 *C*–*E* shows four example pairs of neurons (five repetitive trials; green for VPL raster plots and cyan for S1 raster plots) responding during the first 250 ms after stimulus onset holding feed-forward (Fig. 2*C*), feed-back (Fig. 2*D*), and bidirectional (Fig. 2*E*) information, together with neuron pairs with nonsignificant statistic values (Fig. 2*F*). Since the significance analysis leading to DI is always single-trial, the choice of five trials in Fig. 2*D* is only for illustrative purposes here.

Stimulus Presence Modulates Feed-Forward and Bidirectional Information. Having set the above definitions, we first examined for each type of DI the average DI delay as a putative intrinsic property of each directionality case (*SI Appendix*, Fig. S2). Bidirectional information occurred at shorter delays than unidirectional information for both stimulus-present (trials = 3,217 in neuron pairs = 84, $D = 0.35$, time-average Cohen's d; *SI Appendix*, Fig. S2*A*, *Left*) and stimulus-absent trials (trials = 4,731 in neuron pairs = 84, $D = 0.37$, time-average Cohen's d; *SI Appendix*, Fig. S2*A*, *Right*). The delay histograms (*SI Appendix*, Fig. S2*B*, *Top*) outside the stimulus period or the PWS revealed that these differences were, in general, due to higher percentage of zero-delay couplings (around 33%) in bidirectional information compared with unidirectional information (around 15%). Further, we examined the DI delay distribution during the stimulus period (*SI Appendix*, Fig. S2*B*). We found that the arrival of the stimulus increased the relative amount of bidirectional information at zero delay (from 33 to 49%). However, the relative amount of feed-forward (from 9 to 19%) and feed-back information (from 9 to 15%) was enhanced at 8 ms.

Second, we investigated two main questions regarding feed-forward, feed-back, and bidirectional information: (*i*) What was the contribution of each DI type to a greater amount of VPL → S1 DI observed during the stimulus presence? and (*ii*) What was the contribution of each neuron pair to this effect? Fig. 3*A* depicts the percentages of DI according to their types (feed-forward, feed-back, and bidirectional) for stimulus-present (Fig. 3*A*, *Left*) and stimulus-absent trials (Fig. 3*A*, *Right*) during the time course of the task. The proposed decomposition highlighted the contribution of each type into the directionality differences illustrated in *SI Appendix*, Fig. S1. The increment in the VPL → S1 DI, especially after the stimulus onset, was mainly contributed by feed-forward information (trials = 3,216 in neuron pairs = 84, $P < 0.05$, $H = 0.23$; blue trace in Fig. 3*A*, *Left*) and lesser by the bidirectional information (trials = 3,216, neuron pairs = 84, $P < 0.05$, $H = 0.1$; orange trace in Fig. 3*A*, *Left*). In contrast, the increase in the S1 → VPL direction (*SI Appendix*, Fig. S1) could only be explained by an increase in bidirectional information. Indeed, genuine feed-back information was not significantly modulated during the stimulus presence ($P > 0.05$; red trace in Fig. 3*A*, *Left*). However, for stimulus-absent trials, no DI type showed a significant modulation (trials = 4,271 in neuron pairs = 84, $P > 0.05$; Fig. 3*A*, *Right*).

We then investigated the contribution of each neuron pair to the increment in feed-forward and bidirectional information during the first half of the stimulus period in the stimulus-present trials. To do so, we repeated the analysis of Fig. 3*A* for every VPL–S1 pair and obtained a stimulus-driven effect size per pair. Fig. 3*B* illustrates these results by sorting the neuron pairs independently for each DI type in a descending effect size order. Consistent with our previous findings, there were more neuron pairs exhibiting large stimulus effects in feed-forward and bidirectional information than in feed-back information. Besides that, ~40% (33/84) and 20% (18/84) of the neuron pairs increased the number

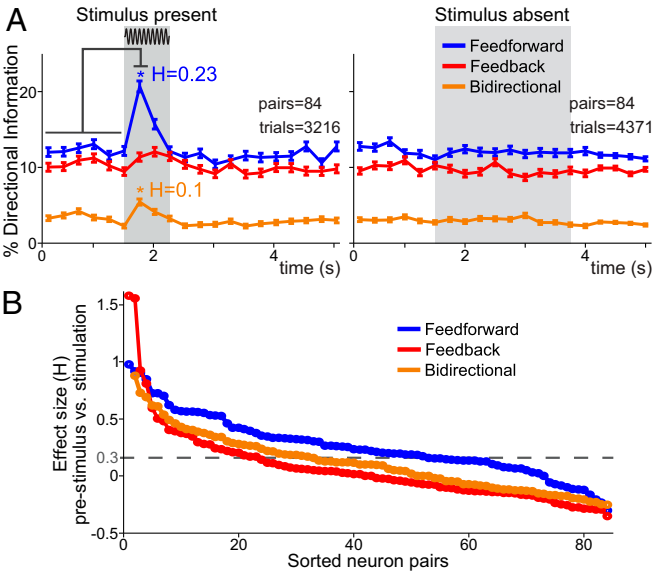

Fig. 3. VPL–S1 feed-forward, feed-back, and bidirectional information during the detection task. We analyzed hit and correct rejection trials across all recorded VPL–S1 neuron pairs. (*A*) Percentage of feed-forward, feed-back, and bidirectional information during the time course of the task during the stimulus-present (*Left*, trials = 3,216 hits; neuron pairs = 84) and stimulus-absent trials (*Right*, trials = 4,371 correct rejections; neuron pairs = 84). Error bars denote the SEM. In all figures, gray boxes depict the stimulus period for the stimulus-present trials and the PWS for the stimulus-absent trials. Asterisks denote significant differences ($P < 0.05$) between the prestimulus (first six task intervals, 1.5 s) and the first half (0 to 0.25 s) of the stimulus period (nonparametric test, $\alpha = 0.05$). H denotes the effect size (Cohen's H) of significant differences. Here and in the next time-varying figures, we removed the variable-time prestimulus period in every stimulus-present trial and aligned all trials to the stimulus onset. In stimulus-absent trials, we aligned the trials to the probe down event (PD). (*B*) Effect size of the difference between the percentage of each DI type during the prestimulus period and during the first stimulus interval as a function of the neuron pairs. Each curve is represented by ordering the neuron pairs in descending order according to the magnitude of the effect size for each particular DI type. The black horizontal dashed line represents the effect size threshold ($H \geq 0.3$).

of feed-forward and bidirectional information, respectively, with moderate and large effect sizes ($H > 0.3$; Fig. 3*B*).

Next, we asked how often a VPL–S1 neuron pair could simultaneously handle both DI modulations during the stimulus period. To address this question, we correlated the stimulus effect sizes associated with each DI type across all of the recorded VPL–S1 neuron pairs. The correlation value between the effect sizes was rather low ($\rho = -0.11$, $P > 0.5$, Spearman's rho), suggesting that feed-forward and bidirectional information might be modulated by a different thalamocortical mechanism. We also analyzed how neuron pairs were differently modulated during stimulus-absent trials (*SI Appendix*, Fig. S3). To this end, we compared the percentage of feed-forward, feed-back, and bidirectional information per neuron pair during the first interval of the stimulus window and during the first interval of the PWS. Each point in *SI Appendix*, Fig. S3 represents a VPL–S1 neuron pair and the histograms of all points' angles with respect to the stimulus-present axis (x axis: stimulus present; y axis: stimulus absent) are shown as insets. Therefore, angular values smaller than 45° indicated a stronger amount of DI during the stimulus period. Thus, mean angular values indicated that the stimulus-present effect ($\theta < 45°$) was more prominently manifested in feed-forward ($\theta = 30.5°$; *SI Appendix*, Fig. S3) and bidirectional information ($\theta = 25.2°$; *SI Appendix*, Fig. S3) than in feed-back information ($\theta = 41.1°$; *SI Appendix*, Fig. S3). In sum, we provided

consistent evidence from independent analyses that tactile stimuli mainly modulated feed-forward and bidirectional information in the VPL–S1 neuron pairs.

Correlation Between the Firing Rate and the Type of Directional Information. The statistical method used in this study infers DI measurements by preserving the firing rate of both sequences in the null distribution, thus avoiding to a large extent the bias introduced by fluctuations of the neuronal spikes (25, 26). To empirically corroborate this fact, we examined the influence of the firing rate into the observed VPL–S1 DI. In previous related work (17, 18) we showed that the average firing rate was larger in VPL than in S1 neurons (Fig. 1*E*). Therefore, the reported increase of feed-forward information (compared with feed-back information) occurred while the VPL and S1 neurons exhibited similar firing rates. This initially suggested a low dependence between the firing rate and the existence of DI. We then tested this hypothesis by correlating the firing rate driver and target neurons with the existence of incoming/outgoing DI (*SI Appendix*). The obtained Spearman correlation coefficients were significant but rather low for both driver (intervals = 206,360 in neuron pairs = 84, $\rho = 0.11$, $P < 0.05$; *SI Appendix*, Fig. S4*A*) and target neurons (intervals = 206,360 in neuron pairs = 84, $\rho = 0.07$, $P < 0.05$; *SI Appendix*, Fig. S4*A*). Moreover, these results were stable during stimulus-absent trials (intervals = 206,280 in neuron pairs = 84, $\rho = 0.1$ for driver spike trains, $\rho = 0.07$ for target spike trains, $P < 0.05$; *SI Appendix*, Fig. S4*B*). This shows that the increase in the number of DI estimates during the stimulus period could not be explained merely by an increase in the mean firing rate of either the VPL or S1 neurons.

The results shown above suggested that the firing rate might be poorly correlated with the distinct DI types. To specifically address this question, we first computed the time-varying correlation (Spearman's rho) between the firing rate in VPL and S1 neurons (*SI Appendix*, Fig. S4 *C* and *D*) associated with feed-forward, feed-back, and bidirectional information for stimulus-present (trials = 3,216 in neuron pairs = 84; *SI Appendix*, Fig. S4 *C* and *D*, *Left*) and stimulus-absent (trials = 4,371 in neuron pairs = 84; *SI Appendix*, Fig. S4 *C* and *D*, *Right*). The results show that the correlation values obtained during the entire time course of the task were upper-bounded by 0.1 for VPL neurons and by 0.2 for S1 neurons. For S1 neurons specifically, the correlation values decreased during the stimulus period. This implies that, for a substantial number of S1 neurons, the reported increase in firing rate (Fig. 1*E*) during the stimulus presence was not accompanied by an increase of incoming/outgoing DI with VPL. Besides, during the stimulus presence, the correlation values were larger for bidirectional information (rather than unidirectional) in VPL and S1 neurons, suggesting that neurons holding bidirectional information were particularly prone to have large firing rates. To further study this question, we examined the firing rate of VPL and S1 neurons associated with feed-forward, feed-back, and bidirectional information (Fig. 4 and *SI Appendix*). Our analysis revealed that the firing rate of VPL and S1 neurons was not significantly different ($n = 53$ and $n = 75$, respectively, Wilcoxon rank-sum test, $P > 0.05$; Fig. 4) between feed-forward and feed-back information across all task intervals, including those from the stimulus period. In contrast, neurons holding bidirectional information showed a significant increase in their firing rate with respect to the unidirectional case during the first interval of the stimulus period ($P < 0.05$; Fig. 4), in agreement with the reported larger correlation observed in the bidirectional type (*SI Appendix*, Fig. S4 *C* and *D*). These increases were manifested at suprathreshold stimulus amplitudes for VPL neurons ($n = 53$, $P < 0.001$; Fig. 4) during the entire stimulus period but for S1 neurons ($n = 75$, $P < 0.05$; Fig. 4) only during the first interval of the stimulus period. Interestingly, for stimulus-absent trials, bidirectional neurons showed enhanced firing

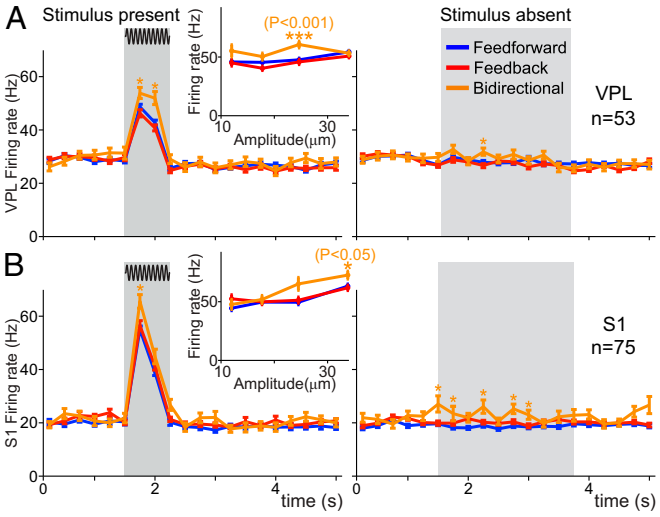

Fig. 4. Mean firing rate of VPL and S1 neurons during the detection task for feed-forward, feed-back, and bidirectional information. We analyzed hit and correct rejection trials across all recorded neurons in VPL and S1. For all panels, gray boxes depict the stimulus period for the stimulus-present trials (*Left*) and the PWS for the stimulus-absent trials (*Right*). Blue, red, and orange traces depict the mean firing rate for neurons holding feed-forward, feed-back, and bidirectional information, respectively, during the time course of the detection task (neuron pairs = 84). Error bars denote the SEM. (*A*) Mean firing rate for VPL neurons ($n = 53$; *Left*, trials = 1,995 hits; *Right*, trials = 2,764 correct rejections). Insets depict the mean firing rate as a function of the stimulus amplitude during the stimulus period. Asterisks denote significant differences (*$P < 0.05$, ***$P < 0.001$, Wilcoxon rank-sum test) among the firing rate of neurons holding distinct DI. (*B*) Similar to *A*, but for S1 neurons ($n = 75$; *Left*, trials = 2,853 hits; *Right*, trials = 3,854 correct rejections).

rates during PWS intervals compared with unidirectional neurons. In sum, these results show that firing rates were not able to discriminate between unidirectional information (feed-forward vs. feed-back) but could be significantly higher for bidirectional information during specific task intervals regardless of the stimulus presence.

Finally, we simulated a stochastic model to evaluate the performance of the DI estimation method as a function of the neuronal firing rate and assess any potential bias in the reported empirical correlations with the firing rate (*SI Appendix*, Fig. S5; details provided in the legend). The results of the model for parameter values that approximated the average firing rate of neurons and the percentage of DI measured in the real data validated that the spurious correlations introduced by the DI estimation method were very low for both unidirectional and bidirectional models (Spearman's rho < 0.08). In the meantime, the DI estimation method was shown to attain large sensitivity values (>90%) even for low firing rates (~35 Hz).

The Amount of VPL–S1 Directional Information Is Modulated by the Stimulus Amplitude. We showed above that both feed-forward and bidirectional VPL–S1 information was enhanced by the stimulus presence, while feed-back information was minimally affected (Fig. 3). Furthermore, each DI type could be modulated by different neuronal populations. This prompted us to hypothesize that feed-forward and bidirectional information could be differently related to the stimulus amplitude. To further investigate this question, we divided the stimulus-present trials into three groups based on the stimulus amplitude. We grouped the 9-μm trials within the near-threshold (Fig. 5*A*, *Top Right*) group and defined the suprathreshold (Fig. 5*A*, *Top Left*) and subthreshold (Fig. 5*A*, *Bottom Left*) groups as those stimulus-present trials above and below 9 μm, respectively. We choose 9 μm as the cutoff amplitude since it is the closer amplitude to the monkey's

mean detection threshold (8 μm; Fig. 1*B*). We also considered stimulus-absent trials for comparison (Fig. 5*A*, Bottom Right). First, we quantified the amount of DI within each group (Fig. 5*A*). Notably, we found that the stimulus effect observed for all amplitudes (Fig. 3*B*) was mainly due to the suprathreshold group (>9 μm). At these amplitudes, feed-forward and bidirectional information showed a significant incremental effect (trials = 2,237 in neuron pairs = 84, $P < 0.01$, $H = 0.26$ and $H = 0.14$; Fig. 5*A*, *Top Left*), while feed-back information was not significantly altered ($P > 0.05$). In contrast, for the near-threshold group, the feed-forward increment was preserved (trials = 443 in neuron pairs = 84, $P < 0.01$, $H = 0.2$; Fig. 5*A*, *Top Right*), while bidirectional information dropped dramatically ($P > 0.05$). Finally, the subthreshold amplitudes only showed a weaker significant increase in the amount of feed-forward information (trials = 536 in neuron pairs = 84, $P < 0.01$, $H = 0.13$; Fig. 5*A*, *Bottom Left*). Thus, the results illustrated in Fig. 5*A* demonstrated that the amount of DI was amplitude-dependent. To examine this dependency, we focused on the first 250 ms of the stimulus-present period and plotted the percentage of DI types as a function of the stimulus amplitude (Fig. 5*B*). In addition, we computed single-trial (r) and average-trial (R) Spearman's rho correlations between the amount of DI and amplitude values (*SI Appendix*). During the first 250 ms the amount of each DI type was correlated with the stimulus amplitude values as measured by single-trial types ($P < 0.05$; Fig. 5*B*). However, when considering average-trial correlations, the significance analysis provided different outcomes across DI types. Indeed, Fig. 5*B* shows that feed-forward (trials = 7,587, $r = 0.12$ in neuron pairs = 84, $R = 0.96$, $P < 0.01$; Fig. 5*B*, *Left*) and bidirectional (trials = 7,587, $r = 0.07$ in neuron pairs = 84, $R = 0.87$, $P < 0.05$; Fig. 5*B*, *Right*) information exhibited a significant monotonic modulation, while feed-back information remained approximately constant over the amplitude values (trials = 7,587, $r = 0.03$ in neuron pairs = 84, R = 0.26, $P > 0.05$; Fig. 5*B*, *Middle*). These effects are further illustrated in *SI Appendix*, Fig. S6 by representing feed-back and bidirectional against feed-forward information, which suggested that the bidirectional trend was mainly driven by suprathreshold amplitudes. These results complemented the analysis of Fig. 5*A*, revealing that the amount of feed-forward and bidirectional information was monotonically associated with the stimulus amplitude. Overall, feed-forward and bidirectional information was enhanced by the stimulus presence and they could convey information about the stimulus amplitude.

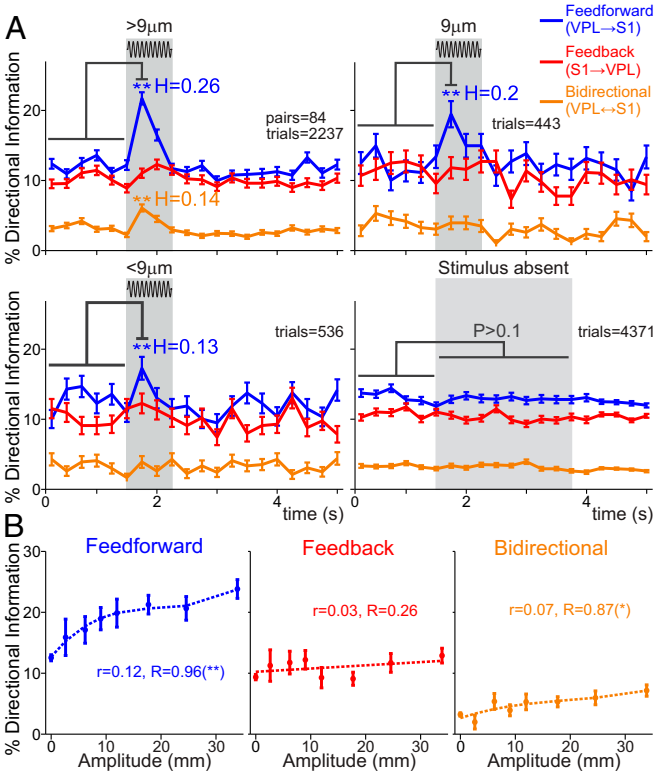

Fig. 5. VPL–S1 feed-forward and bidirectional information is modulated by the stimulus amplitude. We analyzed hit and correct rejection trials across all VPL–S1 neuron pairs. Hit trials were subdivided into three categories (suprathreshold, near threshold, and subthreshold). (*A*) Time course of the percentage of feed-forward (VPL → S1, blue), feed-back (S1 → VPL, red), and bidirectional (S1 ↔ VPL, orange) information between VPL and S1 neurons during stimulus-present and stimulus-absent trials. From left to right and from top to bottom: percentage of DI for suprathreshold (>9 μm, neuron pairs = 84; trials = 2,237 hits; *Top Left*), near threshold (9 μm, neuron pairs = 84; trials = 443 hits; *Top Right*), subthreshold (<9 μm, neuron pairs = 84; trials = 536 hits; *Bottom Left*) stimulus amplitudes, and stimulus-absent trials (neuron pairs = 84; trials = 4,371 correct rejections; *Bottom Right*). Asterisks denote significance levels (**$P < 0.01$; nonparametric test) between the prestimulus (first six task intervals, 1.5 s) and the first half (0 to 0.25 s) of the stimulus period. *H* denotes the effect size (Cohen's *H*) of significant percentage differences. Error bars denote the SEM. (*B*) Mean percentage of feed-forward, feed-back, and bidirectional information as a function of the stimulus amplitude during the first half of the stimulus period (*Left*, 250 ms). The value r is the correlation between the stimulus amplitude and the existence of DI in each type across all trials (no amplitude averages) with Spearman correlation (trials = 7,587). The value R is the analogous correlation considering amplitude-average values (number of stimulus amplitudes = 8). Asterisks depict significance (*$P < 0.05$, **$P < 0.01$, Spearman correlation). Error bars denote the SEM.

Influence of Task Context in Thalamocortical Directional Information. We showed above that for most recorded VPL–S1 neuron pairs there was more feed-forward than feed-back information during the first half (250 ms) of the stimulus-present trials. This differentiated amount of DI was related exclusively to sensory information processing, but whether it was also influenced by the task's context remained unknown. To investigate this question, we applied our directionality analysis to a control task in which the monkey was passively stimulated by the same set of tactile stimuli but no perceptual report was required. Using task-balanced datasets (*SI Appendix*), we repeated some of the previous analyses for stimulus-present trials (neuron pairs = 36, trials = 1,307 hits) and stimulus-absent trials (neuron pairs = 36, trials = 1,364 control rejects) in both task conditions, exploring potential differences in the percentage of DI when the monkey was passively stimulated (Fig. 6). Based on the previous analysis of amplitude modulation (Fig. 5), we restricted our analysis during stimulus-present trials to near-threshold and suprathreshold amplitudes for feed-forward information (neuron pairs = 36, trials = 1,105 hits) and suprathreshold amplitudes for feed-back and bidirectional information (neuron pairs = 36, trials = 932 hits).

We first revisited the firing rate of single neurons in VPL and S1 (17, 18) and found that the average (over neurons) firing rate of each area was not substantially altered during the time course of the passive stimulation task (Fig. 6*A*). Consistent with this quantification, we thereafter analyzed the percentage of DI during the passive condition over all neuron pairs that had been recorded in both task conditions. For these paired samples, we outlined task intervals where the difference was significant and the effect size was larger than 0.3. In general, our analysis revealed task-specific variations at the level of DI, which occurred around the stimulus period for stimulus-present trials (Fig. 6 *B–D*, *Left*). Compared with the vibrotactile task, the arrival of the (suprathreshold) stimulus in passive trials produced a lesser increase of bidirectional information (neuron pairs = 36; Fig. 6*D*, *Left*) during the second half of the stimulus window and a specific increase of feed-back information during the first 250 ms

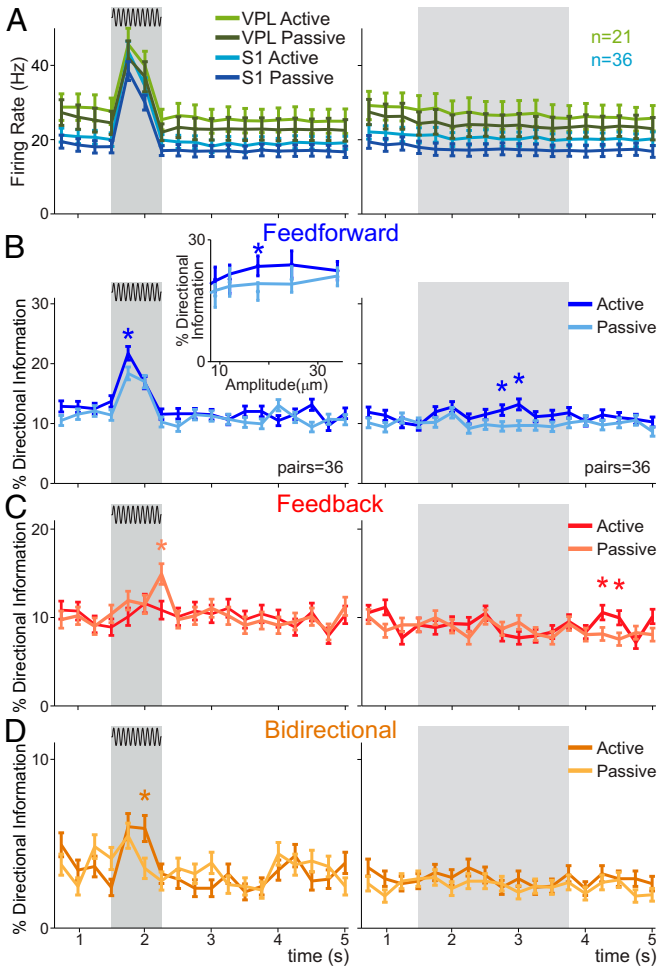

Fig. 6. VPL–S1 DI during passive stimulation. For the comparison between the vibrotactile detection task and the passive stimulation task, we analyzed supra- and near-threshold hit trials for feed-forward information and suprathreshold hit trials for feed-back and bidirectional information in addition to correct rejection trials. The left panels depict stimulus-present trials, whereas the right side depict stimulus-absent trials. Dark and light colors depict DI data belonging to the active and passive conditions, respectively. (*A*) Time course of the mean firing rates for VPL (n = 21) and S1 (n = 36) neurons. The same neuron pairs (pairs = 36) were simultaneously recorded during the detection task and passive stimulation. (*B*) Time course of the percentage of feed-forward information (pairs = 36; trials = 1,105 hits; trials = 1,364 correct rejections). (*Inset*) The percentage of feed-forward information as a function of stimulus amplitude. (*C*) Percentage of feed-back information for the active and passive conditions across time (pairs = 36; trials = 932 hits; trials = 1,364 correct rejections). (*D*) Percentage of bidirectional information across time (pairs = 36; trials = 932 hits; trials = 1,364 correct rejections). Asterisks denote significance levels (*P < 0.05, nonparametric balanced test) associated with effect sizes (Cohen's H) larger than 0.3.

of the poststimulation window (neuron pairs = 36; Fig. 6*C*, *Left*). Notably, feed-forward information was significantly higher in the active than the passive condition, both during the stimulus period (Fig. 6*B*, *Left*) and PWS (Fig. 6*B*, *Right*). Thus, our findings show that DI across VPL–S1 neuron pairs was sensitive to the task context. In particular, passive stimulation mitigated the amount of bidirectional information during stimulus delivery while enhancing feed-back information with a certain delay.

Influence of the Task on Zero-Lag Interactions. A priori, we defined DI types by matching the location of driver or target neurons to either VPL, S1, or both. However, the characterization of each DI type presented in *SI Appendix*, Fig. S2 unraveled features that could give rise to new characterizations. More specifically, the large percentage of bidirectional information occurring at zero delay (≥33%; *SI Appendix*, Fig. S2*B*) suggested that the zero-delay case could partially explain the trends reported for the bidirectional type. To study this question in detail, we decomposed bidirectional information into two subtypes: zero lag, for which both DI statistics (one per direction) were significant at zero delay, and non-zero lag, for which both statistics were simultaneously significant at non-zero delays (*SI Appendix*). We repeated most of the previous analyses on these two subtypes (Fig. 7). To begin with, we represented the time-varying percentage of each DI subtype during the time course of the task (Fig. 7*A*). Crucially, Fig. 7*A* shows that only zero-lag bidirectional information was significantly increased during the first 250 ms of the stimulus period ($P < 0.05$, $H > 0.14$; Fig. 7*A*, *Left*) and hence the reported overall bidirectional increase ($H = 0.1$; Fig. 7*A*, *Left*) was due to the zero-delay subtype. We then related zero-lag and non-zero lag bidirectional information with the firing rate of neurons in VPL and S1 ($n = 53$ and $n = 75$, respectively; Fig. 7 *B* and *C*). The results highlight that the firing rate of neurons holding zero-lag bidirectional information was frequently larger than those with non-zero lag (Wilcoxon rank-sum test, $P < 0.05$). Nonetheless, *SI Appendix*, Fig. S7 *A* and *B* validated that this enhancement of the firing rate did not simply follow from a larger correlation between the firing rate and zero-lag bidirectional information compared with other DI types (Spearman's rho < 0.2). Another reported feature of bidirectional information was its monotonic association with the stimulus amplitude (Fig. 5 and *SI Appendix*, Fig. S7*C*, *Left*). Hence, in light of the new decomposition, we investigated the contribution of the zero-lag sub-type to this trend. Performing the same analysis of Fig. 5*B*, we found that the modulation of bidirectional information by the stimulus amplitude was mostly explained by zero-lag bidirectional information (trials = 7,587, r = 0.06 in neuron pairs = 84, $R = 0.81$, $P < 0.05$; *SI Appendix*, Fig. S7*B*). Finally, we investigated the influence of the task context into zero-lag bidirectional information (Fig. 7*D*). In line with our previous analysis (Fig. 6*D*), we considered suprathreshold amplitudes (neuron pairs = 36, trials = 932 hits) and compared the amount of zero-lag bidirectional information across the same neurons pairs in both tasks. Critically, as compared to the original task ($P < 0.05$), zero-lag bidirectional information was not altered by the stimulus presence during passive stimulation. In contrast, this context effect was not observed in non-zero-lag bidirectional information. Taken together, we concluded that the distinctive features of bidirectional information reported so far were essentially occurring at zero delay. For the sake of interpretability, zero-lag bidirectional information will be referred to hereafter in short as zero-lag interaction.

Feed-Forward Information Correlates with the Animal's Task Performance. An important question is whether the DI across VPL–S1 neuron pairs is modulated by the animal's task performance. To further examine this question, we first analyzed the differences between hit and miss trials during the stimulus-present condition (Fig. 8*A*, *Left*) and between correct rejections and false-alarm trials during stimulus-absent trials (Fig. 8*A*, *Right*) across single neuron firing rates (Fig. 8*A*) and DI types (Fig. 8 *B*–*D*). In stimulus-present trials, we controlled for the effect of stimulus amplitudes by analyzing the difference between hits and misses at the near-threshold amplitude value (9 μm), where the number of samples was the most balanced between hit (trials = 443 hits in neuron pairs = 79) and miss responses (trials = 389 misses in neuron pairs = 79). In both experimental conditions, we controlled for a possible sample bias and experimental sessions effect, by using group-based permutation tests at the level of neuron pairs (*SI Appendix*). We then outlined task

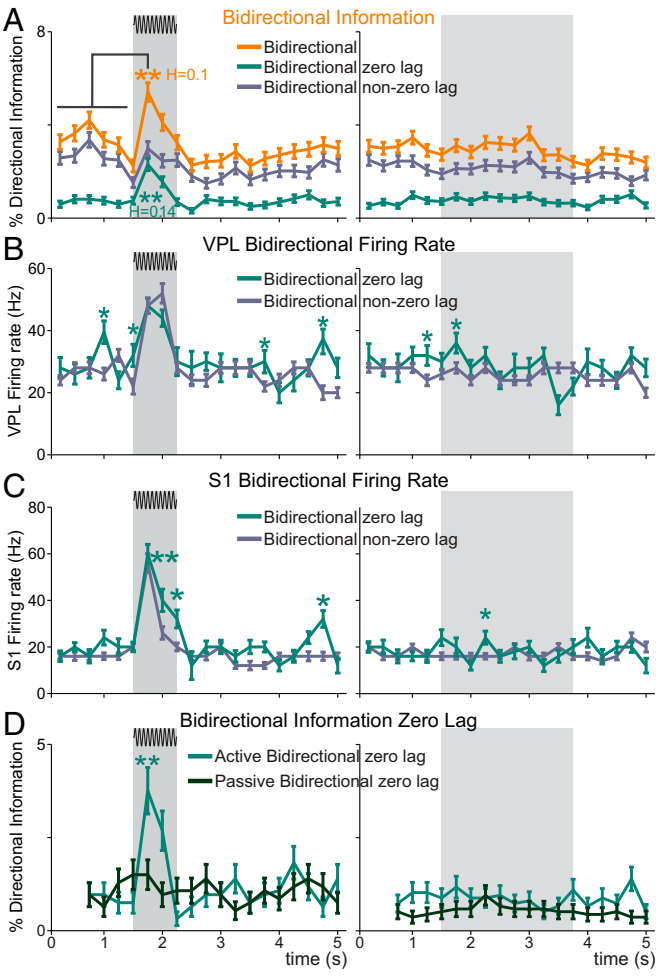

Fig. 7. Bidirectional information across zero-lag and non-zero-lag trials. We analyzed suprathreshold hit and correct rejection (CR) trials across neuron pairs. Error bars denote the SEM. (*A*) Percentage of overall bidirectional information (pairs = 84), zero-lag, and non-zero-lag bidirectional information across the task during stimulus-present (*Left*, trials = 3,216 hits) and stimulus-absent trials (*Right*, trials = 4,371 CR). Asterisks denote significant differences (**$P < 0.01$, nonparametric test) between the prestimulus (first six task intervals, 1.5 s) and the first half (0 to 0.25 s) of the stimulus period. H denotes the effect size (Cohen's *H*) of significant differences. (*B*) Mean firing rate for VPL neurons ($n = 53$; *Left*, trials = 1,995 hits; *Right*, trials = 2,764 CR). Asterisks denote significant differences (*$P < 0.05$; **$P < 0.01$; Wilcoxon rank-sum test) among the firing rate of neurons holding zero-lag and non-zero-lag bidirectional information. (*C*) Similar to *B*, but for S1 neurons ($n = 75$; *Left*, trials = 2,853 hits; *Right*, trials = 3,854 CR). (*D*) Percentage of zero-lag and non-zero-lag bidirectional information during suprathreshold and stimulus-absent trials (n pairs = 36; trials = 932 hits; trials = 1,364 CR) across the detection task and passive stimulation. Asterisks denote significance levels (**$P < 0.01$; nonparametric balanced test) associated with effect sizes (Cohen's *H*) larger than 0.3.

intervals where the difference was significant and the effect size was larger than 0.2. Our analysis primarily revealed that the amount of feed-forward information during the first half of the stimulus period in stimulus-present trials was significantly larger ($P < 0.05$, $H > 0.2$) in hit trials (Fig. 8*A*, *Left*). In contrast, our data did not unravel strong significant differences between correct rejections and false alarms during stimulus-absent trials (trials = 4,188 correct rejections and false alarm trials = 933 in neuron pairs = 82; Fig. 8*A*, *Right*). Overall, our results indicate that the amount of feed-forward information during the first half of the stimulus window was correlated with the monkey's behavior and could potentially predict the monkey's performance in stimulus-present trials (Fig. 8*B*, *Left*).

Discussion

Here, we sought to determine the functional roles of thalamocortical information flows in perception at a fine temporal scale. This was done by estimating a directional information measure (referred to as DI) between simultaneously recorded VPL–S1 neuron pairs sharing the same cutaneous receptive field while monkeys performed a vibrotactile detection task. Notably, the estimated DI could not be merely explained by increases in the firing rates of neurons within VPL or S1 during the stimulus period. We found that the stimulus presence elicited a significant increment on the amount of feed-forward information (VPL → S1) and zero-lag interaction. In

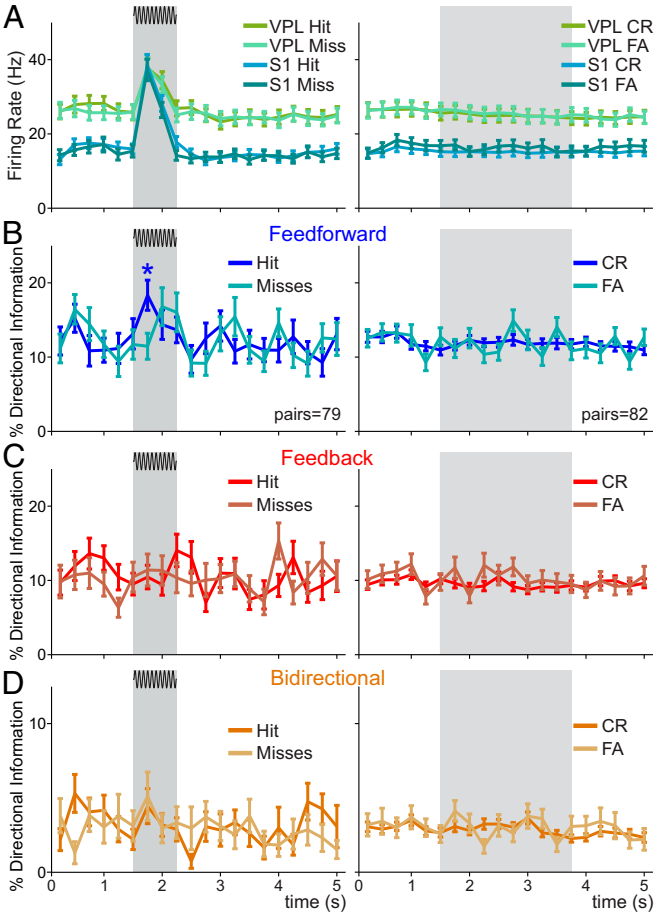

Fig. 8. VPL–S1 DI during correct and error trials. We analyzed hit and miss trials for near-threshold (9 μm) amplitudes as well as correct rejection trials and false alarms across all VPL–S1 neuron pairs. (*A*) Time course of the mean firing rate VPL ($n = 48$) and S1 ($n = 70$) neurons during stimulus-present trials and for VPL ($n = 51$) and S1 ($n = 73$) neurons during stimulus-absent trials. Neuronal responses were separated according to the monkey's behavioral output. (*Left*) Hits and misses for the stimulus-present trials. (*Right*) Correct rejections and false alarms for stimulus-absent trials. Neurons and pairs were selected to have more than two trials at near-threshold amplitude for each condition. (*B*) Time course for the percentage of feed-forward information. (*C*) Time course for the percentage of feed-back information. (*D*) Time course for the percentage of bidirectional information. (*B–D*, *Left*) Hits (dark colors) and misses (light colors) for the stimulus-present trials (neuron pairs = 79; trials = 443 hits; trials = 389 misses). (*B–D*, *Right*) Correct rejections (dark colors) and false alarms (light colors) for the stimulus-absent trials (neuron pairs = 82; trials = 4,188 correct rejections; trials = 933 false alarms). Asterisk denotes significance level (*$P < 0.05$; nonparametric test) associated with effect sizes (Cohen's *H*) larger than 0.2.

contrast, pure feed-back (S1 → VPL) information remained practically unaltered during the stimulus presence. Remarkably, increments in feed-forward and zero-lag interaction were differently modulated as a function of the stimulus amplitude. Specifically, we found a monotonic relationship between both feed-forward and zero-lag interaction and the stimulus amplitude. However, zero-lag interaction only emerged significantly with suprathreshold sensory inputs during task performance. Additionally, we identified that thalamic and cortical neurons involved in bidirectional information exhibited higher firing rates during stimulus presence. Interestingly, the amount of feed-forward information was correlated with the monkeys' performance when they judged the presence at near-threshold stimuli. Also, during a passive stimulation task, when the monkeys were not required to report their percepts, both feed-forward and, more prominently, zero-lag interaction were reduced during the stimulus presence. This suggests that feed-forward information and zero-lag interaction are modulated by the task context. We discuss these findings below.

In the current study, we extended previous spectral and neural population studies on thalamocortical directionality (10, 27–29) to the temporal domain, at the level of single-neuron activity. To achieve this, we analyzed the DI between VPL and S1 neuronal spike trains with a nonlinear measure (5, 20, 21). Indeed, we decomposed single-neuron DI into three types, feed-forward, feed-back, and bidirectional, and explored their temporal evolution from the prestimulus up to the poststimulus intervals of the detection task. In particular, the lack of pure feed-back modulation (i.e., not concurrent to feed-forward information) during the stimulus period suggests that the spike-field coherence increment in the S1 → VPL direction shown in ref. 29 could be associated with increments in zero-lag interaction. Our data analysis approach involved the use of nonparametric significance tests (30) and the choice of the percentage of significant DI estimates as a relevant connectivity metric (5). Both choices were critical to detect nonlinear spike-train temporal correlations in a way that was shown to be weakly dependent on the firing rate in real and simulated data. As a result, we were able to analyze neuronal data in a dimension that was quasi-orthogonal to the firing rates (17, 18), while still showing rich stimulus modulations. It is important to mention the differences between the DI measure used here and the widespread measure of noise correlation (31, 32). Noise correlation averages across trials under the same stimulus condition, correlating fluctuations in firing rate of two neurons. In contrast, DI quantifies, in a single trial and for any given time, the information that the recent past and present spike train of a given neuron has about the present spike train of the other, simultaneously recorded, neuron.

Notably, feed-forward VPL–S1 information was modulated during the stimulus period. Further, the modulation was stronger 250 ms immediately after the stimulus onset. These findings are congruent with the adaptation of feed-forward information over the stimulus period. Indeed, previous studies have shown that thalamic and cortical neurons become adapted to tactile stimuli after several pulses (17, 18, 33). Moreover, it has been reported that this adaptation changes the neural code of cortical neurons and thalamic synchrony from a detection to a discrimination modality (34). As stated above, our directionality measure is poorly correlated with differences in firing rate of VPL and S1 neurons. Therefore, our results are congruent with the adaptive coding paradigm (34), by showing that feed-forward and zero-lag interactions exhibit the strongest modulation during the first part of the stimulus presence. In sum, we hypothesize that feed-forward adaptation reflects an internal mechanism that prioritizes the information contained within the first pulses of the sinusoidal stimulus to further transmit this information to the cortex and, therefore, for stimulus detection during this task.

According to the standard classification of thalamic sensory nuclei (6), VPL is considered a first-order relay nucleus that mainly transmits afferent information to S1 in the presence of cortical feedback (9, 35, 36). Our results support this view by showing that feed-forward information alone was primarily boosted during the first 250 ms immediately after the stimulus onset. The increment in feed-forward information was concentrated at a delay of 8 ms, which is consistent with previous literature (37). Moreover, these increments were reduced during incorrect trials and, to a lesser extent, during the passive control condition. In particular, the relationship between feed-forward information and the monkey's performance during stimulus-present trials is of special novelty. In previous related studies, this correlation did not arise either in spiking activity (18) or in the oscillatory activity (29). This result suggests that perceptual detection might be related to the amount of stimulus information flowing from VPL to S1. In contrast, pure feed-back information did not display substantial task modulations. We hypothesize that pure feed-back information might be relevant for perceptual detection but is generally less frequent than feed-forward information. However, cortical areas and higher-order thalamic nuclei (reviewed in ref. 38) might show more prominent feed-back corticothalamic information, perhaps related not only to facilitating the gating of the stimulus but also to some other cognitive aspects not detected in this task (however, see the discussion below).

Our study revealed that feed-back information could take place concurrently with feed-forward information, suggesting the emergence of a thalamocortical loop, denominated here in sum as bidirectional information. In particular, our analysis identified that bidirectional information showed bimodality between those cases where DI simultaneously occurred at zero delay (zero-lag interaction) and those cases at non-zero delay. Crucially, only zero-lag interaction was modulated by the stimulus presence, involved neurons exhibiting higher firing rates than in the unidirectional case, and was significantly diminished in the passive stimulation task. Hence, zero-lag interaction conveyed both stimulus and contextual information, thus indicating that its mechanism might be different from the non-zero subtype. Unlike the feed-forward type, we suggest that zero-lag interaction may not reflect direct routing of information (39). Instead, it could be established by common inputs from mediating cortical neurons. In particular, it will be interesting in future studies to simultaneously record the activity of higher-order areas like prefrontal cortex to examine how common cortical inputs driving zero-lag interactions (40) are associated with the expectancy caused by different prestimulus period times, a variable that was out of the scope of this study. In light of the existing models of corticothalamic circuitry (ref. 7 and Fig. 1), we hypothesize that the inferred feed-forward thalamocortical information could be related to layer 4 (15) as well as deep cortical layers 5/6 in S1 (41). In fact, future experiments involving multicontact electrodes and inactivation are needed to shed light on the contribution of the distinct cortical layers to the information flow within the thalamocortical circuit. However, we consider that the task-context modulation of zero-lag interaction requires the engagement of downstream cortical areas in this loop. Specifically, in concordance with computational models supporting zero-lag brain interarea synchronization (42–44), we propose that zero-lag interaction could be originated by a top-down modulation of cortical areas, establishing a similarly delayed reciprocal loop with both S1 and the thalamus (9, 45).

Recently, a study in monkeys performing a visual detection task was also able to relate the propagation of neural activity along the visual pathway with the monkey's detection accuracy (46). The authors showed that information about unreported stimuli may be lost at any stage of the pathway (V1–V4–prefrontal cortex) with an overall excursion that depended on the stimulus strength. Despite the methodological differences with the study presented here [the authors recorded cortical areas along the visual

pathway, analyzed multiunit activity (MUA) instead of single-unit activity, indirectly measured activity propagation via local MUA, and used microstimulation, among others], their results suggest that stimulus perception of near-threshold stimuli may depend on the feed-forward information flow across the early stages of the sensory pathway. More specifically, they explain their results with a model involving thalamocortical and corticocortical propagation, but no corticothalamic projections. While our main findings may fit in this model (see also ref. 3), the task modulation of zero-lag interaction between VPL and S1 suggests the additional existence of indirect corticothalamic pathways toward VPL in the somatosensory model.

In brief, the present study employed a fine-temporal methodology supporting that the increment of VPL → S1 neuronal DI (as opposed to S1 → VPL) at around 8 ms during the stimulus period reflects the effective transmission of tactile information from thalamus to cortex. Moreover, it suggests that the amount of feed-forward information occurring during the first 250 ms of stimulation correlates with the monkey's stimulus perception and with the behavioral task performance. Meanwhile, zero-lag interaction, which was reduced when monkeys were not required to report stimulus presence, may reflect the top-down modulation of the corticothalamic circuitry needed for stimulus perception. Our results, therefore, contribute to understanding the DI functional flow between the VPL and S1 during the detection of a tactile stimulus. Finally, the minimalistic approach used here, that is, the simultaneous recording of VPL–S1 neuron pairs sharing the same receptive field, together with the estimation of DI flow, could be used not only to investigate the functional role of the thalamocortical DI during perception but also across other brain areas in this and other behavioral tasks.

Materials and Methods

Monkeys were trained to report whether or not they felt the stimulus (*SI Appendix*). Neuronal recordings were obtained in VPL and S1 while the monkeys performed the detection task. Directional information was calculated between neuron pairs simultaneously recorded in VPL and S1 (*SI Appendix*). Animals were handled in accordance with standards of the National Institutes of Health and Society for Neuroscience. All protocols were approved by the Institutional Animal Care and Use Committee of the Instituto de Fisiología Celular, Universidad Nacional Autónoma de México.

ACKNOWLEDGMENTS. This work was supported by Dirección General de Asuntos del Personal Académico de la Universidad Nacional Autónoma de México Grants PAPIIT- IN202716 and PAPIIT-IN210819, Consejo Nacional de Ciencia y Tecnología Grant 240892 (to R.R.), Spanish Research Project PSI2016-75688-P [Agencia Estatal de Investigación/Fondo Europeo de Desarrollo Regional (AEI/FEDER), European Union] (to G.D.), by the European Union's Horizon 2020 Research and Innovation Programme under Grants 720270 [Human Brain Project Specific Grant Agreement 1 (HBP SGA1)] and 785907 (HBP SGA2) (to G.D.), and by the Catalan Agència de Gestió d'Ajuts Universitaris i de Recerca (AGAUR) Programme 2017 Suport als Grups de Recerca (SGR) 1545 (to G.D.). Y.V. was supported by a Pew Latin American Fellowship and a Charles H. Revson Biomedical Science Fellowship.

1. Salinas E, Hernández A, Zainos A, Romo R (2000) Periodicity and firing rate as candidate neural codes for the frequency of vibrotactile stimuli. *J Neurosci* 20:5503–5515.
2. de Lafuente V, Romo R (2005) Neuronal correlates of subjective sensory experience. *Nat Neurosci* 8:1698–1703.
3. de Lafuente V, Romo R (2006) Neural correlate of subjective sensory experience gradually builds up across cortical areas. *Proc Natl Acad Sci USA* 103:14266–14271.
4. Hernández A, et al. (2010) Decoding a perceptual decision process across cortex. *Neuron* 66:300–314.
5. Tauste Campo A, et al. (2015) Task-driven intra- and interarea communications in primate cerebral cortex. *Proc Natl Acad Sci USA* 112:4761–4766.
6. Sherman SM (2016) Thalamus plays a central role in ongoing cortical functioning. *Nat Neurosci* 19:533–541.
7. Alitto HJ, Usrey WM (2003) Corticothalamic feedback and sensory processing. *Curr Opin Neurobiol* 13:440–445.
8. Briggs F, Usrey WM (2007) A fast, reciprocal pathway between the lateral geniculate nucleus and visual cortex in the macaque monkey. *J Neurosci* 27:5431–5436.
9. Crandall SR, Cruikshank SJ, Connors BW (2015) A corticothalamic switch: Controlling the thalamus with dynamic synapses. *Neuron* 86:768–782.
10. Wang JY, et al. (2007) Corticofugal influences on thalamic neurons during nociceptive transmission in awake rats. *Synapse* 61:335–342.
11. Jones EG (2002) Thalamic circuitry and thalamocortical synchrony. *Philos Trans R Soc Lond B Biol Sci* 357:1659–1673.
12. Sherman SM, Guillery RW (2006) *Exploring the Thalamus and Its Role in Cortical Function* (MIT Press, Cambridge, MA).
13. Alonso JM, Usrey WM, Reid RC (1996) Precisely correlated firing in cells of the lateral geniculate nucleus. *Nature* 383:815–819.
14. Ahissar E, Sosnik R, Haidarliu S (2000) Transformation from temporal to rate coding in a somatosensory thalamocortical pathway. *Nature* 406:302–306.
15. Bruno RM, Sakmann B (2006) Cortex is driven by weak but synchronously active thalamocortical synapses. *Science* 312:1622–1627.
16. Bruno RM (2011) Synchrony in sensation. *Curr Opin Neurobiol* 21:701–708.
17. Vázquez Y, Zainos A, Alvarez M, Salinas E, Romo R (2012) Neural coding and perceptual detection in the primate somatosensory thalamus. *Proc Natl Acad Sci USA* 109:15006–15011.
18. Vázquez Y, Salinas E, Romo R (2013) Transformation of the neural code for tactile detection from thalamus to cortex. *Proc Natl Acad Sci USA* 110:E2635–E2644.
19. Carnevale F, de Lafuente V, Romo R, Barak O, Parga N (2015) Dynamic control of response criterion in premotor cortex during perceptual detection under temporal uncertainty. *Neuron* 86:1067–1077.
20. Massey J (1990) Causality, feedback and directed information. *Proceedings of International Symposium on Information Theory and its Applications* (Institute of Electronics, Information and Communication Engineers, Tokyo), pp 27–30.
21. Jiao J, Permuter HH, Zhao L, Kim YH, Weissman T (2013) Universal estimation of directed information. *IEEE Trans Inf Theory* 59:6220–6242.
22. Winkler AM, Ridgway GR, Webster MA, Smith SM, Nichols TE (2014) Permutation inference for the general linear model. *Neuroimage* 92:381–397.
23. Cohen J (1988) Statistical power analysis for the behavioral sciences. *Stat Power Anal Behav Sci* 2:567.
24. Deschênes M, Veinante P, Zhang ZW (1998) The organization of corticothalamic projections: Reciprocity versus parity. *Brain Res Brain Res Rev* 28:286–308.
25. Pipa G, Wheeler DW, Singer W, Nikolić D (2008) NeuroXidence: Reliable and efficient analysis of an excess or deficiency of joint-spike events. *J Comput Neurosci* 25:64–88.
26. Louis S, Gerstein GL, Grün S, Diesmann M (2010) Surrogate spike train generation through dithering in operational time. *Front Comput Neurosci* 4:127.
27. Fitzgerald TH, Valentin A, Selway R, Richardson MP (2013) Cross-frequency coupling within and between the human thalamus and neocortex. *Front Hum Neurosci* 7:84.
28. Bastos AM, Briggs F, Alitto HJ, Mangun GR, Usrey WM (2014) Simultaneous recordings from the primary visual cortex and lateral geniculate nucleus reveal rhythmic interactions and a cortical source for γ-band oscillations. *J Neurosci* 34:7639–7644.
29. Haegens S, et al. (2014) Thalamocortical rhythms during a vibrotactile detection task. *Proc Natl Acad Sci USA* 111:E1797–E1805.
30. Gilson M, Tauste Campo A, Chen X, Thiele A, Deco G (2017) Nonparametric test for connectivity detection in multivariate autoregressive networks and application to multiunit activity data. *Netw Neurosci* 1:357–380.
31. Ecker AS, et al. (2014) State dependence of noise correlations in macaque primary visual cortex. *Neuron* 82:235–248.
32. Kohn A, Coen-Cagli R, Kanitscheider I, Pouget A (2016) Correlations and neuronal population information. *Annu Rev Neurosci* 39:237–256.
33. Khatri V, Hartings JA, Simons DJ (2004) Adaptation in thalamic barreloid and cortical barrel neurons to periodic whisker deflections varying in frequency and velocity. *J Neurophysiol* 92:3244–3254.
34. Wang Q, Webber RM, Stanley GB (2010) Thalamic synchrony and the adaptive gating of information flow to cortex. *Nat Neurosci* 13:1534–1541.
35. Blomquist P, et al. (2009) Estimation of thalamocortical and intracortical network models from joint thalamic single-electrode and cortical laminar-electrode recordings in the rat barrel system. *PLoS Comput Biol* 5:e1000328.
36. Ahissar E, Oram T (2015) Thalamic relay or cortico-thalamic processing? Old question, new answers. *Cereb Cortex* 25:845–848.
37. Briggs F, Usrey WM (2008) Emerging views of corticothalamic function. *Curr Opin Neurobiol* 18:403–407.
38. Halassa MM, Kastner S (2017) Thalamic functions in distributed cognitive control. *Nat Neurosci* 20:1669–1679.
39. Besserve M, Lowe SC, Logothetis NK, Schölkopf B, Panzeri S (2015) Shifts of gamma phase across primary visual cortical sites reflect dynamic stimulus-modulated information transfer. *PLoS Biol* 13:e1002257.
40. Riehle A, Grün S, Diesmann M, Aertsen A (1997) Spike synchronization and rate modulation differentially involved in motor cortical function. *Science* 278:1950–1953.
41. Constantinople CM, Bruno RM (2013) Deep cortical layers are activated directly by thalamus. *Science* 340:1591–1594.
42. Fischer I, et al. (2006) Zero-lag long-range synchronization via dynamical relaying. *Phys Rev Lett* 97:123902.
43. Vicente R, Gollo LL, Mirasso CR, Fischer I, Pipa G (2008) Dynamical relaying can yield zero time lag neuronal synchrony despite long conduction delays. *Proc Natl Acad Sci USA* 105:17157–17162.
44. Gollo LL, Mirasso C, Sporns O, Breakspear M (2014) Mechanisms of zero-lag synchronization in cortical motifs. *PLoS Comput Biol* 10:e1003548.
45. Collins DP, Anastasiades PG, Marlin JJ, Carter AG (2018) Reciprocal circtuits linking prefrontal cortex with ventral and dorsal thalamic nuclei. *Neuron* 98:366–379.e4.
46. van Vugt B, et al. (2018) The threshold for conscious report: Signal loss and response bias in visual and frontal cortex. *Science* 360:537–542.